

are obtained from experiments. The static crystalline parameters are usually determined from the optical spectra, but in CaF_2 the optical spectra are complicated by the presence of satellite lines, and by the existence of local fields of different symmetries due to charge compensation. If the ground state is Γ_8 , and if Γ_8 occurs

more than once in the decomposition of the ground J manifold, the wave functions may be determined from the spin-resonance experiments. Some of the wave functions and a survey of crystalline-field parameters for rare-earth ions in CaF_2 are given in the first article of Ref. 24.

Effective Mass of Positrons in Metals

D. R. HAMANN

Bell Telephone Laboratories, Murray Hill, New Jersey

(Received 22 December 1965)

The self-energy of a positron in an electron gas due to electron-positron correlations is calculated to the lowest order in the dynamically screened interaction. It is shown that the dressed positron quasiparticle can be described by an effective mass, but that the calculated effective mass is much too small to account for that measured by observing thermal effects in positron-annihilation experiments. Corrections due to more complicated self-energy processes and to electron-exchange interactions are estimated and found to be small.

1. INTRODUCTION

POSITRON annihilation has been studied as a means of gaining information about the band structure of metals. In addition, however, such experiments provide an example of a distinguishable test charge interacting with a many-electron system, and we shall deal here with a particular feature of the correlations in this combined system.

The possibility of studying low-energy aspects of positron annihilation arises from the fact that the positron lifetime is long compared to the time it takes a positron injected into a metal to reach equilibrium with the electrons.¹ Suppose we naively neglect all interactions and consider an electron gas at 0°K containing a positron in its zero-momentum state. The two gamma rays produced when the positron annihilates with one of the electrons will carry away just the momentum of that electron. Angular-correlation measurements of the z component of the momentum of each gamma-ray pair should then give a distribution equal to that of the z components of the electron momenta—an inverted parabola with a cutoff at $k_z = k_F$ ($\hbar = 1$). Now suppose this system is heated. The positron will have a Maxwellian velocity distribution, and its average momentum will be $(T/T_F)^{1/2}k_F$. The average increase in momentum for electrons at the Fermi surface will be $(T/T_F)k_F$, so for a typical T of 10²°K and T_F of 10⁵°K, the thermal smearing of the momentum-distribution cutoff will be due almost entirely to the momentum of the positron.

In actual metals, observed positron lifetimes are an order of magnitude shorter than those predicted by

the noninteracting model.¹ This suggests that the interaction profoundly disturbs the momentum distribution of electrons in the vicinity of the positron. It is a paradox of this problem that the momentum fluctuations of the electrons and positron cancel in just such a way that the observed momentum distributions (from simple s - p conduction bands) reproduce almost exactly the parabola of the naive model. Kahana and co-workers have calculated the interaction effects on both the lifetime and the momentum distribution, and have obtained reasonable agreement with experimental observations in several approximations.² In considering the thermal smearing of the momentum distribution cutoff, we can completely avoid the complexities of these calculations by the following argument: Since the correlation effects do, in fact, cancel in the momentum distribution, only the average momentum of the positron as it undergoes various virtual transitions enters into the thermal smearing. The quasiparticle formed by the positron and its screening cloud of electrons will have a Boltzmann distribution in energy. Therefore, calculating the quasiparticle E -versus- k relationship (which hopefully may be expressed by an effective mass) should permit a complete description of the thermal smearing. This physical argument is supplemented by the recent work of Majumdar, which establishes with great generality the existence of a sharp break in the gamma-ray momentum distribution at 0°K, and the possibility of measuring the positron effective mass through the thermal smearing of this break.³ One experiment of this sort has been carried

¹ R. A. Ferrell, *Rev. Mod. Phys.* **28**, 308 (1956).

² S. Kahana, *Phys. Rev.* **117**, 123 (1960); **129**, 1622 (1963); J. P. Carbotte and S. Kahana, *ibid.* **139**, A213 (1965).

³ C. K. Majumdar, *Phys. Rev.* **140**, A227 (1965); **140**, A237 (1965).

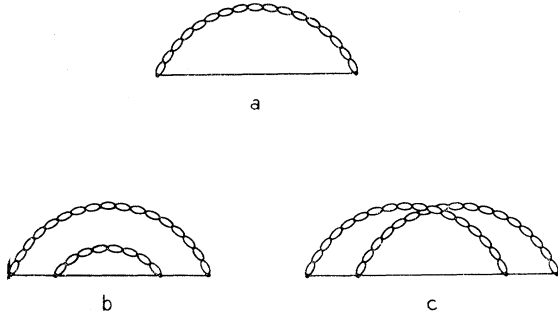


FIG. 1. Positron self-energy diagrams. The solid line is the bare-positron Green's function, and the "bubble" line is the screened Coulomb interaction.

out for sodium, and an effective mass of $(1.9 \pm 0.4)m$ found.⁴

The positron interacts with the ions as well as with the conduction electrons. It thus possesses its own set of energy bands, which are not simply related to the electron bands since the ion cores repel the positron, and since its wavefunction is not orthogonal to those of the core electrons. We wish to calculate only the electron correlation contribution to the positron m^* , and shall neglect both band-structure effects and phonon effects.

2. THE POSITRON SELF-ENERGY

We shall use a zero-temperature Green's-function formalism to calculate the positron self-energy.⁵ This procedure is justified since the energy scale in the correlation processes is set by the electron-gas Fermi energy. The bare-positron Green's function is given by

$$G^0(\mathbf{k}, \omega) = (\omega - \epsilon_{\mathbf{k}} + i\delta)^{-1}, \quad (1)$$

and the complete Green's function by

$$G(\mathbf{k}, \omega) = [\omega - \epsilon_{\mathbf{k}} - \Sigma(\mathbf{k}, \omega)]^{-1}, \quad (2)$$

where $\epsilon_{\mathbf{k}} = k^2/2m$, and Σ is the self-energy. We note that the imaginary infinitesimal in (1) and the imaginary part of Σ in (2) are always positive since the Fermi energy for the positron is zero. The simplest physically meaningful self-energy diagram is shown in Fig. 1(a). The string of bubbles represents the infinite sum of the bare Coulomb interaction line and the Coulomb interaction with arbitrary numbers of electron-hole "bubble" polarization diagrams inserted. The straight line is G^0 . This is the same approximation used to calculate the electron quasiparticle self-energy by Quinn and Ferrell.⁶ Diagrams such as those shown in Figs. 1(b) and 1(c) are of higher order in the screened interaction and will be neglected. In addition, we shall neglect exchange

⁴ A. J. Stewart and J. B. Shand, *Bull. Am. Phys. Soc.* **10**, 21 (1965); *Phys. Rev. Letters* **16**, 261 (1966).

⁵ See, for example, A. A. Abrikosov, L. P. Gorkov, and I. E. Dzyaloshinski, *Methods of Quantum Field Theory in Statistical Physics*, translated by R. A. Silverman (Prentice-Hall, Inc., Englewood Cliffs, New Jersey, 1963).

⁶ J. Quinn and R. A. Ferrell, *Phys. Rev.* **113**, 812 (1958).

corrections to the screening, despite the fact that their contribution may be important at metallic densities.⁷ It will later be seen that the inclusion of such corrections would be premature at this point.

The analytic expression of the self-energy of Fig. 1(a) is

$$\Sigma(\mathbf{k}, \omega) = \frac{i}{(2\pi)^4} \int d^3\mathbf{q} \, d\omega' G^0(\mathbf{k} - \mathbf{q}, \omega - \omega') \frac{v(q)}{\epsilon(q, \omega')}, \quad (3)$$

where $v(q) = 4\pi e^2/q^2$, and $\epsilon(q, \omega')$ is the propagating dielectric function in the self-consistent-field approximation.⁸ The ω' integration is most conveniently carried out by using a spectral representation for the interaction propagator,

$$\frac{v(q)}{\epsilon(q, \omega)} = v(q) + \frac{1}{\pi} \int_0^\infty dt \left| \text{Im} \frac{v(q)}{\epsilon(q, t)} \right| \times \left[\frac{1}{\omega - t + i\delta} - \frac{1}{\omega + t - i\delta} \right]. \quad (4)$$

When (4) is substituted in (3), the $v(q)$ term gives zero because the ω' contour must be closed in the lower half plane for reasons of causality,⁵ excluding the pole of G^0 . The order of the ω' and t integrations may be interchanged in the remaining term, since the position of the poles of the integrand relative to the contours is well defined, and the ω' contour closed in either half plane. This gives

$$\Sigma(\mathbf{k}, \omega) = \frac{1}{8\pi^4} \int d^3\mathbf{q} \int_0^\infty dt \left| \text{Im} \frac{v(q)}{\epsilon(q, t)} \right| \frac{1}{\omega - \epsilon_{\mathbf{k}-\mathbf{q}} - t + i\delta}. \quad (5)$$

The quasiparticle energy is given by the real part of ω at the pole of the analytic continuation of $G(\mathbf{k}, \omega)$ nearest the real axis. To a first approximation this is

$$E_{\mathbf{k}} = \epsilon_{\mathbf{k}} + \text{Re} \Sigma(\mathbf{k}, \epsilon_{\mathbf{k}}) = \epsilon_{\mathbf{k}} + \frac{1}{8\pi^4} \int d^3\mathbf{q} P \int_0^\infty dt \left| \text{Im} \frac{v(q)}{\epsilon(q, t)} \right| \frac{1}{\epsilon_{\mathbf{k}} - \epsilon_{\mathbf{k}-\mathbf{q}} - t}, \quad (6)$$

where P denotes Cauchy principal value.⁹

3. ANALYTIC PROPERTIES OF QUASIPARTICLE ENERGY

If we change to the dimensionless variables $\mathbf{y} = \mathbf{k}/k_F$, $\mathbf{x} = \mathbf{q}/k_F$ and $u = t/(k_F^2/2m)$, express $E_{\mathbf{k}}$ in units of $k_F^2/2m$, and use spherical coordinates for the \mathbf{x} inte-

⁷ J. Hubbard, *Proc. Roy. Soc. (London)* **A243**, 336 (1957).

⁸ J. Lindhard, *Kgl. Danske Videnskab. Selskab, Mat. Fys. Medd.* **28**, No. 8 (1954).

⁹ The same result can be found by using a canonical transformation to decouple the positron from the electron gas, and averaging over the electron-gas ground state. See D. R. Hamann and A. W. Overhauser [*Phys. Rev.* **143**, 183 (1966)], Eq. (23), dropping the diagonal exchange term.

gration, we find

$$E_y = y^2 + \frac{2}{\pi^2 a_0 k_F} \int_0^\infty dx \int_{-1}^1 d\xi \times P \int_0^\infty du \left| \operatorname{Im} \frac{1}{\epsilon(x,u)} \right| \frac{1}{2xy\xi - x^2 - u}, \quad (7)$$

where $\xi = \cos\theta$ and a_0 is the first Bohr radius. Now since we want the effective mass, it is tempting to expand the integrand in (7) in a power series in $y\xi$, carry out the ξ integration, and then pick out the coefficient of y^2 . This procedure yields

$$E_y = y^2 - \frac{2}{\pi^2 a_0 k_F} \sum_{j=0}^\infty \frac{y^{2j} 2^{2j+1}}{2j+1} \times \int_0^\infty dx \int_0^\infty du \left| \operatorname{Im} \frac{1}{\epsilon(x,u)} \right| \frac{x^{2j}}{(x^2+u)^{2j+1}}. \quad (8)$$

The principal value has been dropped since the integrands are not singular within the range of integration. However, they are suspiciously singular at $x=u=0$, and it is doubtful if any of the coefficients exist above $j=0$. It is necessary to study the analytic properties of E_y more carefully to determine what portion, if any, of the small- y expansion (8) is valid. Returning to (7), if we fix ξ and consider the remaining integrals to define a function of y as a complex variable, we see that this function has a branch point at $y=0$, and a cut running along the positive or negative real axis (for ξ positive or negative). Therefore, a power-series expansion such as (8) about $y=0$ does not exist.

To determine the nature of the branch point, we must perform some approximate analytic evaluation of (7), carrying out the integrations in the indicated order. $\operatorname{Im} \epsilon^{-1}(x,u)$ contains a smoothly varying continuum portion, and a delta function at the plasma pole. Since the plasma u is finite, it can be shown from (7) that only the continuum portion will effect the branch point. The dielectric function is given by

$$\begin{aligned} \epsilon(x,u) = & 1 + \frac{1}{\pi a_0 k_F x^3} \left[(1-r^2) \ln \left| \frac{1+r}{1-r} \right| + 2r \right. \\ & + (1-s^2) \ln \left| \frac{1+s}{1-s} \right| + 2s + i\pi(1-r^2)\theta(1-r^2) \\ & \left. - i\pi(1-s^2)\theta(1-s^2) \right], \\ r = & \frac{1}{2}(x-u/x), \\ s = & \frac{1}{2}(x+u/x), \end{aligned} \quad (9)$$

where θ is the unit step function. One must be extremely careful approximating $\epsilon(x,u)$ in the small x and u limit, since its real part can approach either plus or minus infinity, depending on the order in which the limits are

taken. An adequate limiting form which retains these analytic features is

$$\epsilon(x,xz) \xrightarrow[x \rightarrow 0]{z \rightarrow 0} 1 + (4/\pi a_0 k_F x^2) (1 - \frac{2}{3}z^2 - \frac{1}{4}\pi iz). \quad (10)$$

The corresponding form of $\operatorname{Im} \epsilon^{-1}$, correct to first order in z , is

$$\operatorname{Im} \epsilon^{-1}(x,xz) = (z/a_0 k_F x^2) (1 + 4/\pi a_0 k_F x^2)^{-2}. \quad (11)$$

The continuum portion of the u integral in (7) runs from $u_1 = \operatorname{Max}(0, x^2 - 2x)$ to $u_2 = x^2 + 2x$, as may be seen by examining the imaginary part of (9). For the present purpose, it is adequate to take $\operatorname{Im} \epsilon^{-1}$ to be equal to (11), $u_1=0$, and $u_2=2x$ for all x . This replaces $\operatorname{Im} \epsilon^{-1}$ by a "triangular" approximation in u which is correct for small u/x , is larger than the true function for intermediate u/x , but which "compensates" by going to zero sooner. Making these approximations, the variable change $u=x\xi$, and introducing the parameter $\gamma^2 = 4/\pi a_0 k_F$, the continuum portion of (7) is

$$I_c \approx \frac{\pi\gamma^4}{8} \int_0^\infty dx \int_{-1}^1 d\xi \frac{x^2}{(x^2+\gamma^2)^2} P \int_0^{2x} d\xi \frac{\xi}{(2y\xi - x - \xi)}. \quad (12)$$

The ξ integration is easily carried out, and we find

$$\begin{aligned} I_c \approx & \operatorname{const} + (\pi\gamma^4/8) \int_0^\infty dx x^2 (x^2+\gamma^2)^{-2} \int_{-1}^1 d\xi (2y\xi - x) \\ & \times [\ln |2y\xi - x| - \ln |2y\xi - x - 2|]. \end{aligned} \quad (13)$$

It is clear that the second term in brackets in (13) will not contribute to the $y=0$ branch point, so we will drop it. After performing the ξ integration, the remaining contribution is

$$I_c' = (\pi\gamma^4/32y) \int_0^\infty dx x^2 (x^2+\gamma^2)^{-2} [(2y-x)^2 \ln |2y-x| - (2y+x)^2 \ln |2y+x|]. \quad (14)$$

This integral is rather complicated, so we will replace $(x^2+\gamma^2)^{-2}$ by γ^{-4} , and terminate the x integration at $x=\gamma$. (The term from the upper limit does not contribute to the branch point at $y=0$ anyway.) Finally, we find the term we seek to be

$$I_c'' = (\pi/15)y^4 \ln |y|. \quad (15)$$

This is the only part of the original expression (7) which does not possess a series expansion about $y=0$. We note that (for real y) its second derivative exists and is equal to zero. Therefore the y^2 term in the series expansions of the portions of (7) we dropped or "approximated away" dominates E_y for y sufficiently small, and we can define a meaningful effective-mass approximation. Equation (15) also implies that while the coefficient of the y^2 term in (8) exists, that of the y^4 term does not. This series is thus asymptotic in a restricted sense.

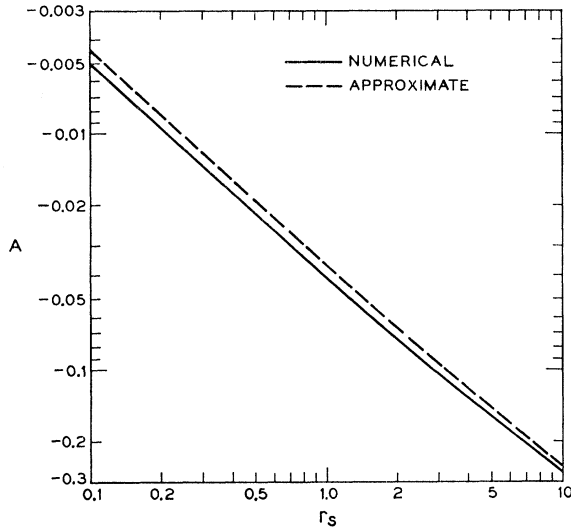


FIG. 2. Numerical and approximate analytic results for the coefficient of the momentum squared in the quasiparticle self-energy versus r_s .

4. EVALUATION OF EFFECTIVE MASS

From (8), we see that the coefficient of the y^2 term is

$$A = \frac{-16}{3\pi^2 a_0 k_F} \int_0^\infty dx \left[\int_{u_1}^{u_2} du \frac{x^2}{(x^2+u)^3} \left| \text{Im} \frac{1}{\epsilon(x,u)} \right| + \frac{x^2 r_p(x)}{[x^2+u_p(x)]^3} \right], \quad (16)$$

where we have explicitly separated the contribution from the plasma pole at $u_p(x)$ with residue $r_p(x)$. This expression was evaluated numerically using the exact functions throughout. Before discussing these results, however, we will discuss an approximate analytic evaluation of (16).

For the continuum portion of (16), we will use the approximate form for $\text{Im} \epsilon^{-1}$ discussed in the last section. This yields the expression

$$A_c \approx (\gamma^4/3) \int_0^\infty dx x^2 (x^2+\gamma^2)^{-2} \int_0^2 d\zeta \zeta / (x+\zeta)^3. \quad (17)$$

We note that the $1/(x+\zeta)^3$ term weights small x and ζ values heavily, and it is for these values that our approximations are exact. The ζ integral is elementary, and we find

$$A_c \approx (\gamma^4/6) \int_0^\infty dx \frac{x^2}{(x^2+\gamma^2)^2} \left[\frac{1}{x} - \frac{x+4}{(x+2)^2} \right]. \quad (18)$$

The first term in the brackets comes from the $\zeta=0$ limit, and the x integral involving it is simple. The other term can be put into elementary form by a tedious but straightforward partial-fraction expansion. The final

result is

$$A_c \approx \gamma^2/12 - (1/6)(4+\gamma^2)^{-3} [16\pi\gamma^3 + 24\gamma^4 \ln\gamma^2 + (40-48 \ln 2)\gamma^4 - 12\pi\gamma^5 - 2\gamma^6 \ln\gamma^2 + (12+4 \ln 2)\gamma^6 + \gamma^8/2]. \quad (19)$$

We note that the leading term in γ^2 comes from the $\zeta=0$, $x=0$ "corner" of the 2-dimensional integration, and that the complicated term from regions where our approximations are poorer involves γ^3 and higher powers. Since $\gamma^2 \propto (1/k_F) \propto r_s$, this approximation scheme gives the correct high-density limit for A_c , a gratifying although unexpected (the author must admit) bonus.

The plasma portion of (16) was approximately evaluated by taking $u_p(x) \approx u_p(0) = 4(3\pi a_0 k_F)^{-1/2}$, and $r_p(x) \approx r_p(0) = (\pi/2)u_p(0)$. The value of x for which cutoff occurs is found in the numerical calculation by comparing $u_p(x)$ to $u_2 = 2x + x^2$, the upper bound of the continuum. An estimate of this was made by taking $u_p(x) \approx u_p(0)$ and $u_2 \approx 2x$, in the hope that neglecting the x^2 term in u_2 would tend to cancel the neglect of dispersion in u_p . The integral is then elementary and we find

$$A_p = \frac{u_0^2}{3} \left[\frac{u_0-4}{4(u_0+4)^2} + \frac{1}{8u_0^{1/2}} \tan^{-1}(\frac{1}{2}u_0^{1/2}) \right], \quad (20)$$

where $u_0 = u_p(0)$. The quantity in brackets goes to zero as u_0 ($\propto r_s^{1/2}$) goes to zero, so the continuum term dominates in the high density limit, where it is exact.

The effective mass is given by

$$m^*/m = 1/(1+A_c+A_p). \quad (21)$$

The numerical results and the analytic approximation for $A = A_c + A_p$ are shown in Fig. 2 as a function of r_s . The approximation is surprisingly good in the metallic density range, which we had no right to expect. The effective mass is shown in Fig. 3, and although we have plotted only the numerical results, the approximate results are almost identical. For sodium, $r_s = 3.92$, $m^*/m = 1.15$, so our result is far too small to account for the experimentally observed $m^*/m = (1.9 \pm 0.4)$.⁴

Let us now return to the discussion of the basic physical approximation involved in our calculation. Instead of taking only the lowest order term in the screened interaction in the self-energy, we might have included a class of higher order diagrams by making the positron line in Fig. 1(a) a dressed line, which would replace G^0 by G in (3), and make it a nonlinear integral equation for Σ . This procedure would then include Fig. 1(b), and all similar graphs in which no two interaction lines crossed. If we solved this integral equation in the single-pole and effective mass approximation for G , u , and $u_p(x)$ in the cubed denominators in (16) would be multiplied by m^*/m , and the bracketed expression would be multiplied by a factor of m^*/m times

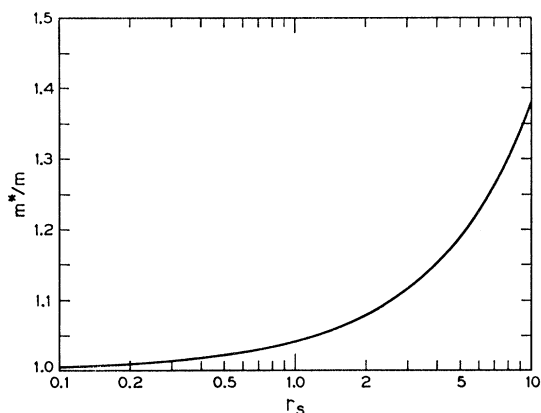


FIG. 3. Quasiparticle effective mass versus r_s .

the renormalization “constant” (the residue at the pole of the analytic continuation of G), which is less than or equal to unity.⁵ An upper bound to the correction which could be expected by this procedure may be obtained by setting the renormalization constant equal to unity and neglecting the m^*/m in the cubed denominators, so

$$m^*/m \leq [1 + A(m^*/m)]^{-1}, \quad (22)$$

where A is the coefficient we have calculated. For $r_s = 3.92$, (22) implies $m^*/m \leq 1.18$, so the correction from graphs of the type of Fig. 1(b) is far too small to account for experiment.

We cannot simply estimate the contribution to Σ from graphs like Fig. 1(c). There is, however, no reason to expect a larger correction from these graphs than from those of Fig. 1(b). Finally, we can estimate the effect of exchange corrections to the electron-gas dielectric function. Hubbard’s approximate prescription replaces $\epsilon(q, \omega)$ with $1 + f(q)[\epsilon(q, \omega) - 1]$, where $f(q)$ is a function which is unity for small q/k_F and $\frac{1}{2}$ for large q/k_F .⁷ Including this in (16) would multiply A by a factor slightly greater than unity but much less than 2 (when the integrations are considered) and would be, again, a small correction.

5. THE CLASSICAL LIMIT

If the recoil term in the energy denominator in (6), $q^2/2m$, is dropped, (7) can be written

$$E_y^c = y^2 + (\pi^2 a_0 k_F)^{-1} \int_0^\infty dx \int_{-1}^1 d\xi P \int_0^\infty du |\text{Im} \epsilon^{-1}(x, u)| \\ \times [1/(2xy\xi - u) - 1/(2xy\xi + u)] \\ + \text{odd function of } \xi]. \quad (23)$$

The odd function of ξ must integrate to zero, and we

may use the spectral representation (4) to show that

$$E_y^c = y^2 + (\pi a_0 k_F)^{-1} \\ \times \int_0^\infty dx \int_{-1}^1 d\xi [\text{Re} \epsilon^{-1}(x, 2xy\xi) - 1]. \quad (24)$$

Ferrell obtained an identical expression by considering a classical point charge moving in an electron gas. His evaluation of the y^2 coefficient in (24) led to an effective-mass correction similar in magnitude to that which we have found.¹⁰

We shall argue that it is not valid to use (24) as an approximate expression in this problem. If one proceeds to expand the integrand in (24) in a power series in y , he finds that the coefficient of y^2 , which involves the second derivative with respect to u of $\epsilon(x, u)$ at $u=0$, has a singularity of the form $(x-2)^{-1}$. It is tempting to impose a principal value and proceed, but the only principal value one is permitted by the theory is “used up” in going from (23) to (24). The difficulty is more basic, however. If we go to the approximate expression for the continuum contribution to the y^2 coefficient, (17), and remove recoil, we see that the integrand for the ξ integration is ξ^{-2} . Therefore the integral diverges at the lower limit, and the coefficient does not exist. Equation (24) can be evaluated, but cannot be a function of y which allows an effective-mass approximation. The recoil in the quantum-mechanical treatment is vital in determining the analytic properties of E_y discussed in Sec. 3.

6. CONCLUSIONS

We have shown that electron-positron correlations cannot by themselves explain the effective mass observed in the thermal smearing of the gamma-ray momentum-distribution edge in sodium.

This implies that the positron band structure must be considered. In particular, the effective mass of the lowest positron band should be calculated. The electron correlations will still help to make the positrons heavier. The effect of phonons on the quasiparticle self-energy may also be relevant, but the positron band calculation would have to be carried out first to obtain the deformation potentials. In addition, a finite-temperature calculation would be needed in this case, since the experiment is carried out well above the Debye temperature.

ACKNOWLEDGMENT

The author is indebted to Dr. A. W. Overhauser for several discussions which led to this calculation.

¹⁰ R. A. Ferrell, University of Maryland, Department of Physics and Astronomy, Technical Report No. 481, 1965 (unpublished) and corrections to this report (private communication).